Journal of Chemical Health Risks

www.jchr.org

JCHR (2024) 14(1), 1111-1120 | ISSN:2251-6727

Design, Synthesis, and Evaluation of Novel 7-(2-hydrazineyl-2-oxoethoxy)-5-hydroxyflavone Derivatives as CDK9 Inhibitors for Targeted Breast Cancer Therapy

N. I. Solanki[a] S.N. Desai[a], R. R. Dedania[b], and Z. R. Dedania[b]

a. Bhagwan Mahavir Center for Advance Research, Bhagwan Mahavir University, Surat, Gujarat, India

b. Bhagwan Mahavir College of Pharmacy, Bhagwan Mahavir University, Surat, Gujarat, India

(Received: 27 October 2023 Revised: 22 November Accepted: 26 December)

KEYWORDS

Breast cancer

CDK9 inhibitors

Flavone derivatives

Molecular docking

ABSTRACT:

Introduction: Across the globe, women face a common adversary in the realm of health: breast cancer, the leading cause of cancer-related deaths among them. Cyclin-dependent Kinase 9 (CDK9) stands at the forefront of gene transcription regulation, playing a pivotal role in the progression of cancerous activities, especially in the difficult-to-treat triple-negative breast cancer (TNBC) subtype. The current research emphasizes the critical demand for better treatments for breast cancer, concentrating on the development and testing of new inhibitors targeting CDK9.

Objectives: In our research, we developed a range of new Flavone-based compounds, focusing on modifications at the C7 position. These compounds feature a variety of pharmacophoric groups, such as dimethyl-pyrazol, mercapto-oxadiazol, mercapto-triazol, and side chains with thiazolidin rings. This approach was aimed at exploring the potential therapeutic effects of these modified Flavone derivatives. These modifications were aimed at enhancing binding affinity to the glycine-rich loop of CDK9, a crucial interaction point in the ATP-binding pocket of the kinase.

Methods: In our study, we advanced the synthesis of novel Flavone derivatives by first converting chrysin into 7-(2-hydrazineyl-2-oxoethoxy)-5-hydroxyflavone, which then underwent cyclo-condensation and Schiff's base reactions. These reactions produced diverse compounds, including dimethyl-pyrazol, mercapto-oxadiazol, and mercapto-triazol derivatives, and a compound with a thiazolidin ring. To evaluate the anticancer properties of these Flavone derivatives, cytotoxicity tests were conducted on two different breast cancer cell lines. We used two types of breast cancer cells for this: one kind that depends on estrogen, known as MCF-7, and another kind that doesn't, known as MDA-MB-231.

Results: The structural characterization of these compounds was confirmed through IR and NMR spectroscopy, revealing the successful incorporation of the intended functional groups and confirming their molecular frameworks. Compounds 4a, 4b, and 4c exhibited potent cytotoxicity against MCF-7 cells, with compounds 4b and 4c also demonstrating significant activity against MDA-MB-231 cells. Molecular docking studies compounds exhibited low root-mean-square displacement (RMSD) values and favorable grid scores, particularly compounds 4b and 4c, indicating efficient binding and stable conformations. The interaction of these derivatives with essential amino acid residues located within the active site of CDK9, especially through hydrogen bonding with CYS 106 was highlighted as a key aspect of their mechanism of action.

Conclusions: Overall, this research contributes to the advancement of breast cancer therapeutics by identifying novel 7-(2-hydrazineyl-2-oxoethoxy)-5-hydroxyflavone-based CDK9 inhibitors with promising anticancer activities. The insights gained from this study hold significant potential for the development of new treatments, particularly for patients with TNBC.

1. Introduction

Breast cancer is the most frequently diagnosed cancer in women across the globe and is the leading cause of cancer deaths in this group. In India, cases of breast cancer are on the rise, especially because of low awareness and limited knowledge in rural

Journal of Chemical Health Risks
www.jchr.org
JCHR (2024) 14(1), 1111-1120 | ISSN:2251-6727

areas [1]. Breast cancer is a diverse illness with five unique molecular subtypes. The luminal subtype of breast cancer, noted for its prevalence, is conventionally managed through endocrine therapy due to its hormone receptor-positive characteristics [2]. However, some individuals develop resistance or develop tolerance to endocrine therapy, reducing their chances of survival [3]. Basal-like breast cancer, frequently identified as triple-negative breast cancer (TNBC), is characterized by its absence of estrogen receptor (ER), progesterone receptor (PR), and human epidermal growth factor receptor-2 (HER2) expression. TNBC is highly diverse and difficult to treat with traditional chemotherapy. TNBC is thought to be more prevalent in India than in other parts of the world [4]. Consequently, there is an urgent need for more potent drugs for breast cancer patients, and this research focuses on discovering compounds that act as direct inhibitors of CDK9.

Important CDK family member CDK9 is a transcription-associated kinase [5]. Cyclin T1 and CDK9 form a heterodimer known as Positive Transcription Elongation Factor-b (P-TEFb) [6]. P-TEFb plays a critical role in transcription elongation through the hyperphosphorylation of Ser2, situated within the heptapeptide sequence in the C-terminal domain of RNA polymerase II (RNAPII). The efficacy of RNA polymerase II (RNAPII) in facilitating transcription is impeded by two primary inhibitors: the DRB-sensitivity inducing factor (DSIF) and the Negative elongation factor (NELF) [7]. CDK9 makes cancer cells resistant to apoptosis by increasing the expression of short-lived anti-apoptotic proteins such as myeloid cell leukemia (Mcl) and X-linked inhibitors of apoptosis protein (XIAP) (Figure 1) [8]. Breast Cancer [9] Prostate cancer [10], neuroblastoma [11], hepatocellular carcinoma [12], lymphoma [13], and osteosarcoma [14] all show significantly increased CDK9 activity [15]. Because of its ability to regulate cellular pathways to start an antitumor response, CDK9 is an interesting cancer treatment target [11].

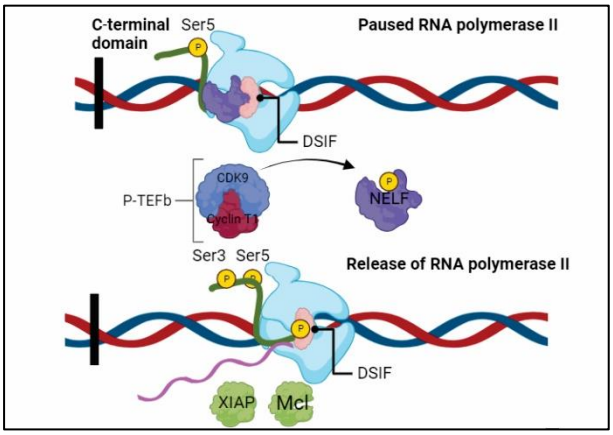

Figure 1. The role of CDK9 in transcription elongation

2. Objective

The main objective of our study is to develop and create new CDK9 inhibitors that exhibit strong anti-cancer effects specifically targeting breast cancer. To achieve this, we'll delve into the crucial binding forces stabilizing existing CDK9 inhibitor Flavopiridol within the ATP-binding pocket of CDK9. In particular, our research will concentrate on investigating the chemical properties around the C7 position on the Flavone structure, aiming to develop effective CDK9 inhibitors. This targeted approach will allow us to introduce diverse pharmacophoric features, such as dimethyl-pyrazol, mercapto-oxadiazol, mercapto-triazol, and a complex thiazolidin ring side chains at the C7 position of the Flavone scaffold. By strategically modifying this key region with these varied ring side chains, we anticipate generating molecules with significantly enhanced binding affinity to the solvent-exposed region of CDK9. This optimized interaction is expected to yield highly effective cancer therapeutics with improved potency and selectivity.

Journal of Chemical Health Risks

www.jchr.org

JCHR (2024) 14(1), 1111-1120 | ISSN:2251-6727

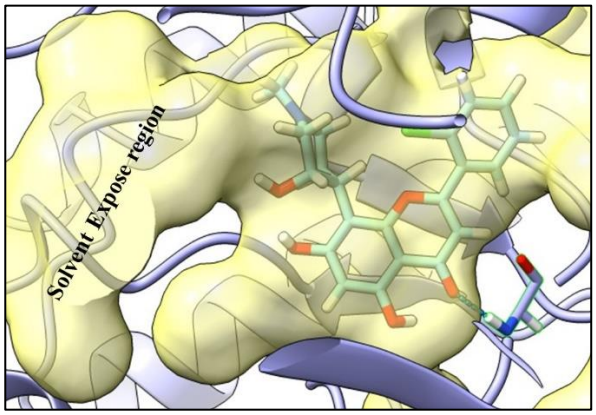

Figure 2. The crystal structure of CDK9, delineated by PDB ID: 3BLR, highlights areas with lower conservation and solvent exposure, suggesting these regions as promising targets for crafting novel CDK9 inhibitors.

3. Methods

3.1. Synthetic Chemistry

In the synthesis of novel flavone derivatives, the process begins with chrysin (1), a natural flavone, which is first converted into 7-(2-methoxy-2-oxoethoxy)-5-hydroxyflavone (2) using methyl 2-bromoacetate under basic conditions [16]. This intermediate is then treated with hydrazine hydrate to yield 7-(2-hydrazineyl-2-oxoethoxy)-5-hydroxyflavone (3a), which serves as a precursor for various derivatives: cyclo-condensation with pentane-2,4-dione produces a dimethyl-pyrazol derivative (4a); reaction with carbon disulfide affords a mercapto-oxadiazol derivative (4b); and using potassium isothiocyanate leads to a mercapto-triazol (4c) derivative. Additionally, Schiff's bases are formed by reacting this intermediate with phenyl isothiocyanate (5a), eventually cyclizing to 7-(2-oxo-2-((4-oxo-2-(phenylimino) thiazolidin-3-yl)amino)ethoxy)-5-hydroxyflavone (6a) (Scheme.1).

Scheme.1. Reagents and conditions: (a) Bromoacetic acid, methyl ester, K_2CO_3 (b) 80% hydrazine hydrate, MeOH (c) acetylacetone, EtOH (d) CS_2, EtOH, KOH (e) KCNS, HCl, EtOH (f) phenyl isothiocyanate, EtOH (g) chloroacetylchloride, CH_3Cl_3.

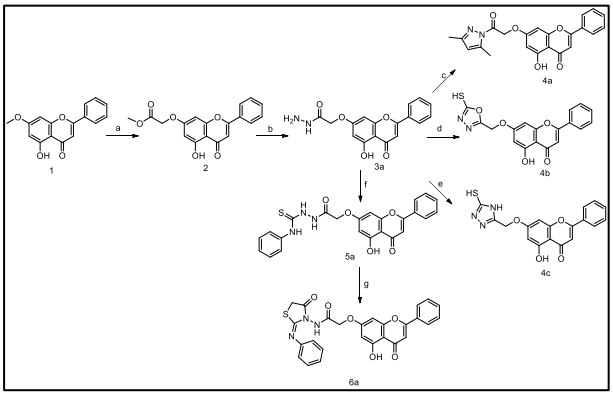

3.1.1. Synthesis of 7-(2-methoxy-2-oxoethoxy)-5-hydroxyflavone

To synthesize 7-(2-methoxy-2-oxoethoxy)-5-hydroxyflavone, the procedure commenced with dissolving 10.6 g (3.93 mmol) of chrysin and 16.3 g (118 mmol) of potassium carbonate in 200 mL of anhydrous DMF. This solution was subsequently cooled to 0°C in an ice bath. Following this, 3.7 mL (3.93 mmol) of methyl 2-bromoacetate was incrementally introduced. The reaction was sustained at 0°C for a duration of 3 hours under continuous stirring. Post-reaction, the mixture was decanted over a mixture of ice and water, energetically stirred to induce precipitate formation. The resulting precipitate was subjected to filtration, followed by washing with water and exposure to air for drying, yielding a yellow powder as the crude product. The purification stage encompassed the use of silica gel column chromatography, employing a chloroform/ethyl acetate mixture in an 8:2 ratio, ultimately acquiring the purified compound, which also presented itself as a yellow powder.

3.1.2. Synthesis of 7-(2-hydrazineyl-2-oxoethoxy)-5-hydroxyflavone (3a)

The synthesis of 7-(2-hydrazineyl-2-oxoethoxy)-5-hydroxyflavone commenced with the cooling of a solution of 7-(2-methoxy-2-oxoethoxy)-5-hydroxyflavone in 300 mL of anhydrous methanol. Subsequently, 5.8 mL (120 mmol) of 100% hydrazine hydrate, along with a controlled quantity of concentrated hydrochloric acid, were methodically added to the cooled solution. This mixture was then subjected to constant stirring for a duration of 1 hour. Upon completion of the reaction,

Journal of Chemical Health Risks
www.jchr.org
JCHR (2024) 14(1), 1111-1120 | ISSN:2251-6727

the mixture was introduced into an ice-water bath, triggering the formation of a solid precipitate. This precipitate was isolated via filtration, followed by a thorough rinsing with water and subsequent air-drying overnight.The final step involved further refinement of the 7-(2-hydrazineyl-2-oxoethoxy)-5-hydroxyflavone to achieve its pure form. This was accomplished using silica gel column chromatography, utilizing a solvent system comprising chloroform and ethyl acetate in an 8:2 ratio. The end product of this process was a fine yellow powder, indicative of the purified compound [17]. Yield: 80% yield; mp: 276 °C; IR (KBr) ν /cm^{-1} 3386, 3067, 2954, 1760, 1670, 1623, 1561, 1393, 1264 and 1140 cm^{-1}; ^{1}H-NMR (500 MHz, $CDCl_3$) δ 7.94 – 7.85 (m, 3H), 7.62 – 7.52 (m, 3H), 6.73 (s, 1H), 6.44 (d, 1H), 6.36 (d, 1H), 4.68 (s, 2H), 3.75 (d, 2H) ^{13}C NMR (125 MHz, $CDCl_3$) δ 182.06, 168.13, 164.42, 163.67, 162.05, 157.91, 131.41, 131.32, 129.19, 126.46, 105.58, 104.63, 97.97, 94.26, 66.22. HRMS (ESI, m/z): calculated for $C_{17}H_{14}N_2O_5$ $[M+H]^+$ 327.0937; *found* 327.5638.

3.1.3. Synthesis of 7-(2-(3,5-dimethyl-1H-pyrazol-1-yl)-2-oxoethoxy)-5-hydroxyflavone (4a)

To synthesize 7-(2-(3,5-dimethyl-1H-pyrazol-1-yl)-2-oxoethoxy)-5-hydroxyflavone (4a), a reaction mixture was initially composed of 3.12 g (10 mmol) of 7-(2-hydrazineyl-2-oxoethoxy)-5-hydroxyflavone, 1.42 g (10 mmol) of acetylacetone, and 10 mL of acetic acid, all within a 100 mL ethanol solvent. This prepared mixture was subjected to reflux for a period of 5 hours. Following the reflux, the mixture was allowed to cool, leading to the formation of a precipitate. This solid product was separated from the mixture through filtration and then underwent recrystallization in ethanol, culminating in the acquisition of the purified compound (4a).Yield: 73 % yield; mp: 259-260 °C; IR (KBr) ν /cm^{-1} 3226, 3145, 2993, 2931, 1760,1721, 1687, 1599, 1564, 1392, 1335, 1232, 1209 and 1132 cm^{-1}; ^{1}H NMR (500 MHz, $CDCl_3$) δ 7.94 –7.87 (m, 2H), 7.62 –7.52 (m, 4H), 6.73 (s, 1H), 6.43 (d, 1H), 6.35 (d, 1H), 6.22 (d, 1H), 5.29 (s, 2H), 2.14 (s, 6H). ^{13}C NMR (125 MHz, $CDCl_3$) δ 182.06, 169.07, 164.08, 163.67, 162.06, 157.91, 151.85, 141.08, 131.41, 131.32, 129.19, 126.46, 111.24, 105.58, 104.63, 98.02, 94.32, 67.77, 14.19, 13.36. HRMS (ESI, m/z): calculated for $C_{22}H_{18}N_2O_5$ $[M+H]^+$ 390.5624; *found* 390.7825.

3.1.4. Synthesis of 7-((5-mercapto-1,3,4-oxadiazol-2-yl)methoxy)-5-hydroxyflavone. (4b)

The synthesis of 7-((5-mercapto-1,3,4-oxadiazol-2-yl)methoxy)-5-hydroxyflavone (4b) was initiated by combining 7-(2-hydrazinyl-2-oxoethoxy)-5-hydroxyflavone (10 mmol) in 150 mL of ethanol with a separately prepared solution of KOH (15 mmol) in 100 mL of ethanol. Following this combination, 200 mL of carbon disulfide was introduced to the mixture, which was then subjected to a reflux process for a duration of 6 hours. Post-reflux, the mixture underwent concentration and was then acidified using diluted hydrochloric acid to induce the formation of a precipitate. This precipitate was collected, thoroughly washed with water, and subsequently underwent recrystallization using a DMFA-H2O mixture. Yield: 76% yield; mp: 234-235 °C; IR (KBr) ν /cm^{-1} 3370, 3091, 3052, 2962, 2929, 1685, 1622, 1602, 1560, 1478, 1405, 1322, 1208, and 1138 cm^{-1} ^{1}H NMR (500 MHz, $CDCl_3$) δ 7.94 – 7.87 (m, 2H), 7.62 – 7.52 (m, 4H), 6.73 (s, 1H), 6.42 (d, 1H), 6.20 (d, 1H), 5.76 (s, 1H), 5.36 (s, 2H). ^{13}C NMR (125 MHz, $CDCl_3$) δ 182.06, 167.19, 163.67, 163.47, 162.05, 157.91, 156.90, 131.41, 131.32, 129.19, 126.46, 105.58, 104.63, 97.92, 94.26, 60.75. HRMS (ESI, m/z): calculated for $C_{18}H_{12}N_2O_5S$ $[M+H]^+$ 369.0656; *found* 369.1527.

3.1.5. Synthesis of 7-((5-mercapto-4H-1,2,4-triazol-3-yl)methoxy)-5-hydroxyflavone (4c)

In the synthesis of 7-((5-mercapto-4H-1,2,4-triazol-3-yl)methoxy)-5-hydroxyflavone (4c), a solution was prepared by dissolving 10 mmol of 7-(2-hydrazinyl-2-oxoethoxy)-5-hydroxyflavone in 100 mL of ethanol. This solution was then subjected to reflux at a temperature of 78°C for 3 hours, in the presence of 2 g of potassium thiocyanate (KSCN, 20.6 mmol) and a small quantity of concentrated hydrochloric acid (HCl). Upon completion of the reaction, the mixture produced a precipitate, designated as compound 4c, which was then isolated using filtration and subsequently dried. Yield: 45 % yield: IR (KBr) ν /cm^{-1} 3386, 3318, 3269, 3063, 2939, 1709, 1680, 1605, 1565, 1397, 1326, 1250 and 1139 cm^{-1}; ^{1}H NMR (500 MHz,

Journal of Chemical Health Risks
www.jchr.org
JCHR (2024) 14(1), 1111-1120 | ISSN:2251-6727

$CDCl_3$) δ 7.94 – 7.87 (m, 3H), 7.62 – 7.52 (m, 4H), 6.98 (s, 1H), 6.73 (s, 1H), 6.40 (d, 1H), 6.19 (d, 1H), 5.17 (s, 2H); ^{13}C NMR (125 MHz, $CDCl_3$) δ 182.06, 164.98, 163.67, 162.98, 162.03, 157.91, 148.57, 131.41, 131.32, 129.19, 126.46, 105.58, 104.63, 97.91, 94.20, 62.85. HRMS (ESI, m/z): calculated for $C_{18}H_{13}N_3O_4S$ $[M+H]^+$ 369.1970; *found* 369.2536.

3.1.6. Synthesis of 7-(2-oxo-2-(2-(phenylcarbono-thioyl)hydrazineyl)ethoxy)-5-hydroxyflavone. (5a)

The synthesis of 7-(2-oxo-2-(2-(phenylcarbonothioyl)-hydrazineyl)ethoxy)-5-hydroxyflavone (5a) was carried out by stirring 10 mmol of 7-(2-hydrazinyl-2-oxoethoxy)-5-hydroxyflavone in 10 mL of ethanol for 24 hours with 1.35 g (10 mmol) of phenyl isothiocyanate and 40 mL of 2 N sodium hydroxide (NaOH, 8 mmol). The procedure continued with the filtration of the mixture, followed by acidification using hydrochloric acid (HCl). This led to the precipitation of the compound, which was subsequently collected and recrystallized from an ethanol/water solution to yield the final product, 5a. Yield: 45 % yield: mp 199-200 °C; IR (KBr) ν /cm^{-1} 3401, 3195, 3052, 2936, 1723, 1680, 1604, 1570, 1516, 1432, 1390, 1307, 1255 and 1132 cm^{-1}; ^1H NMR (500 MHz, $CDCl_3$) δ 9.75 (d, 1H), 9.45 (s, 1H), 7.94 – 7.87 (m, 3H), 7.63 – 7.52 (m, 7H), 7.39 – 7.32 (m, 1H), 7.16 (tt, 1H), 6.73 (s, 1H), 6.44 (d, 1H), 6.36 (d, 1H), 4.55 (s, 2H). ^{13}C NMR (125 MHz, $CDCl_3$) δ 182.06, 180.49, 168.23, 164.46, 163.67, 162.05, 157.91, 141.29, 131.41, 131.32, 129.19, 128.12, 126.87, 126.46, 123.92, 105.58, 104.63, 97.98, 94.28, 66.20. HRMS (ESI, m/z): calculated for $C_{24}H_{19}N_3O_5S$ $[M+H]^+$ 462.1190; *found* 462.3548.

3.1.7. Synthesis of 7-(2-oxo-2-((4-oxo-2-(phenyl-imino)thiazolidin-3-yl)amino)ethoxy)-5-hydroxy-flavone (6a)

To accomplish the synthesis of 7-(2-oxo-2-((4-oxo-2-(phenyl-imino)thiazolidin-3-yl)amino)ethoxy)-5-hydroxy-flavone (6a; 45% yield), a procedure was initiated by dissolving 3.69 g (10 mmol) of 7-(2-oxo-2-(2-(phenylcarbonothioyl)hydrazineyl)-ethoxy)-5-hydroxy-flavone in a solvent mixture consisting of 45 mL of chloroform and 15 mL of ethanol. This solution was subsequently treated with 1.13 g (10 mmol) of chloroacetyl chloride. The reaction mixture was then subjected to a reflux process for a duration of 6 hours. Post-reflux, the solvents were removed under reduced pressure, utilizing equipment such as a rotary evaporator. The resulting residue was then washed with ethanol and water, followed by filtration. Finally, the compound was recrystallized from a DMFA-water solution to obtain the desired product, 6a. Yield: 85 % yield: mp: 273 °C; IR (KBr) ν /cm^{-1} 3240, 3190, 2926, 2905, 1715, 1686, 1609, 1570, 1516, 1433, 1391, 1300, 1256 and 1135 cm^{-1}; ^1H NMR (500 MHz, $CDCl_3$) δ 7.93 – 7.87 (m, 2H), 7.62 – 7.52 (m, 4H), 7.40 – 7.33 (m, 3H), 7.18 – 7.12 (m, 2H), 7.07 (tt, 1H), 6.73 (s, 1H), 6.44 (d, 1H), 6.36 (d, 1H), 4.85 (s, 2H), 3.80 (s, 2H); ^{13}C NMR (125 MHz, $CDCl_3$) δ 182.06, 170.35, 167.09, 164.46, 163.67, 162.05, 157.91, 157.42, 144.94, 131.41, 131.32, 129.75, 129.19, 126.46, 124.17, 121.14, 105.58, 104.63, 98.01, 94.28, 66.54, 31.18. HRMS (ESI, m/z): calculated for $C_{26}H_{19}N_3O_6S$ $[M+H]^+$ 502.1045; *found* 502.4251.

3.2. Cytotoxicity Assay

The MTT test was used to carry out a screening for cytotoxicity, as has been mentioned in earlier research [18]. The breast cancer cell lines MCF-7 and MDA-MB-231, acquired from NCCS Pune, India, were utilized to assess the anticancer efficacy of the synthesized compounds. The experiments were conducted at 37 °C in a 5% CO2 atmosphere, using a medium enriched with 10% fetal bovine serum, 100 IU/ml penicillin, and 100 µg/ml streptomycin. Doxorubicin were dissolved in 0.9% saline and served as controls. The test compounds were prepared in DMSO across various concentrations (50 µg/ml to 0.07 µg/ml). Cells were plated at 5×10^4 cells/mL in 96-well plates and incubated overnight under consistent conditions. After 24 hours, the test and control substances were added. Post overnight incubation, MTT solution was introduced to each well for a 4-hour incubation. Then, DMSO was added to dissolve the formazan, which was measured at 540 nm using a SpectraMax M2e Molecular Devices microplate reader. All tests were done in triplicate, and IC_{50} values were determined using GraphPad Prism 9 software [19].

3.3. Molecular docking

The human CDK9/cyclinT1 complex, with the PDB code: 3BLR, was employed as the structural template for docking studies in our research [20].

Journal of Chemical Health Risks

www.jchr.org

JCHR (2024) 14(1), 1111-1120 | ISSN:2251-6727

This complex was chosen due to its intricate interaction with flavopiridol, a significant component of our study. Ligands were designed using RDKit, an open-source cheminformatics software [21], and optimized with the MMFF94 force field [22]. In our molecular docking studies, we used the Dock6.5 program, targeting a 10.0 Å radius surrounding the ligand's coordinates at the receptor's active site [23]. This process included flexible conformation and energy calculations, with validation based on a ligand root-mean-square displacement (RMSD) value of 2.0 Å. Post-docking analyses were performed using UCSF ChimeraX [24] and LigPlot [25].

4. Results and Discussion

4.1. Synthetic Chemistry

7-(2-Hydrazinyl-2-Oxoethoxy)-5-Hydroxyflavone **(3a),** synthesized from chrysin with a 75% yield, exhibited IR spectral peaks of N-H stretching at 3317 cm^{-1} and carbonyl stretching at 1760 cm^{-1}. Amide groups were indicated by peaks in the 1621-1670 cm^{-1} range. The ^1H NMR spectrum further confirmed its structure with singlets at δ 7.86 ppm (–NH) and δ 4.68 ppm ($–CH_2$).

7-(2-(3,5-dimethyl-pyrazol-1-yl)-2-oxoethoxy)-5-Hydroxyflavone **(4a)** displayed IR spectral peaks of C-H stretches in methyl groups at 2994 cm^{-1}. The ^1H NMR spectrum revealed aromatic protons between δ 7.94-6.22, complemented by methyl carbon peaks in the ^{13}C NMR spectrum at δ 14.19.

7-((5-Mercapto-1,3,4-oxadiazol-2-yl)Methoxy)-5-Hydroxyflavone **(4b)** showed IR spectral peaks for a hydroxy group at 3370 cm^{-1} and a carbonyl group at 1685 cm^{-1}. The ^1H NMR spectrum exhibited aromatic protons at 7.94-7.87 ppm and a potential mercapto SH at 5.76 ppm. The ^{13}C NMR spectrum identified a carbonyl carbon at 182.06 ppm and a methoxy group at 60.75 ppm.

7-((5-Mercapto-4H-1,2,4-triazole-2-yl)Methoxy)-5-Hydroxyflavone **(4c)** exhibited IR spectral peaks of N-H stretches at 3269 cm^{-1}, carbonyl stretches at 1709 cm^{-1}, and aromatic C=C stretches at 1605 cm^{-1}. Aromatic protons were evident in the ^1H NMR spectrum at 7.94-7.52 ppm, with a triazole ring proton at 6.73 ppm. The ^{13}C NMR spectrum supported this structure with a carbonyl peak at 182.06 ppm and an alkoxy signal at 62.85 ppm.

7-(2-Oxo-2-(2-(Phenylcarbonothioyl)Hydrazineyl)-Ethoxy)-5-Hydroxyflavone **(5a)** showed IR spectral peaks of N-H stretches at 3401 and carbonyl stretches at 1723. The ^1H NMR spectrum featured highly deshielded protons of N-H at δ 9.75 and δ 9.45, along with methylene protons in the ethoxy chain at δ 4.55. The ^{13}C NMR spectrum showed carbonyl signals at δ 182.06 and δ 180.49, and an ethoxy carbon signal at δ 66.20.

7-(2-oxo-2-((4-oxo-2-(phenylimino)thiazolidin-3-yl)amino)ethoxy)-5-hydroxyflavone **(6a)** displayed IR spectral peaks of N-H stretching at 3440 cm^{-1}, and carbonyl stretching at 1715, with aromatic C=C stretches at 1609 cm^{-1}. The ^1H NMR spectrum revealed aromatic protons at δ 7.93–7.52, and protons on the thiazolidin ring at δ 6.73, 6.44, and 6.36. Ethoxy group protons appeared as singlets at δ 4.85 and δ 3.80, with the ^{13}C NMR spectrum confirming carbonyl carbons at δ 182.06 and ethoxy carbons at δ 66.54 and δ 31.18.

4.2. Cytotoxicity Assay

The study assessed the anticancer potential of synthetic Flavone derivatives against two breast cancer cell lines: the estrogen-dependent MCF-7 and the estrogen-independent MDA-MB-231 (Table 1). The efficacy of these compounds was benchmarked against the cytotoxic agent doxorubicin, which had IC_{50} values of 1.26 µM for MCF-7 and 4.53 µM for MDA-MB-231 cells. Among the tested compounds, 4a, 4b, and 4c showed significant cytotoxicity against MCF-7 cells, with 4b and 4c also demonstrating effectiveness against MDA-MB-231 cells. In contrast, compounds 3a, 5a, and 6a did not exhibit cytotoxicity in either cell line. The introduction of pyrazol, oxadiazol, and triazol groups at the C7 position on the Flavone scaffold increased hydrophobicity, which enhanced the interactions with target proteins and anticancer activity. However, bulky groups at the C7 position could hinder binding to the target protein, reducing the compound's effectiveness.

Table 1. IC_{50} Values Determined for Flavone Derivatives in MCF7 and MDA-MB-231 Cell Lines

Compound	MCF-7 (µM)	MDA-MB-231 (µM)
3a	>50	>50

Journal of Chemical Health Risks

www.jchr.org

JCHR (2024) 14(1), 1111-1120 | ISSN:2251-6727

4a	23.51±3	>50
4b	11.23±1	4.56±1
4c	18.82±2	6.21±1
5a	>50	>50
6a	>50	>50
Doxorubicin	1.26	4.53

4.3. Molecular docking

The active site of the receptor was identified using the primary coordinates of the native ligand. This was achieved by selecting a cluster sphere that matched the coordinates where the native ligand binds to the receptor's active site. The comparison of docking poses against each native ligand CPB yielded favorable root-mean-square displacement (RMSD) values of 0.234 Å, suggesting accurate alignment with the crystal structure of the native ligands. The redocking process, incorporating flexible conformations, achieved a grid score of -46.201321 kJ/mol for the native ligand CPB. Additionally, the hydrogen bond interaction with CYS 106 in the hinge region was noted as a crucial factor for ligand-receptor interactions. Using the coordinates obtained from redocking, the Flavone derivatives were docked to the receptor, demonstrating promising conformations with low grid score values (Table 2.). Among the various Flavone derivatives studied, compound 4b stood out due to its excellent binding efficiency, characterized by the lowest energy.

conformation. This derivative was observed to form hydrogen bonds with CYS 104 and LYS 48, a feature that was also noted in the 4c derivative (Figure 3). However, it's important to note that the 5a and 6a ligands did not exhibit hydrogen bonding with CYS 104, suggesting a difference in their binding mechanisms or affinities.

Table 2. Flavone Derivatives with the Highest Minimum Grid Scores and Associated Residues in Molecular Docking Analysis

ligand	grid score (kJ. mol^{-1})	Interacted Amino Acid Residues	H-bonding residues	H-bonding Distance
CPB	-46.20	ILE 25, GLY 28, ALA 46, PHE 103, PHE 105, CYS 106, GLU 107, ASP 109, ALA 153, ASN 154, LEU 156	CYS 106	3.03
3a	-41.03	ILE 25, VAL 33, ALA 46, LYS 48, PHE 103, PHE 105, CYS 106, ASP 109, LEU 156, ASP 167	CYS 106 ASP 167	2.99 3.22
4a	-44.28	ILE 25, GLY 28, VAL 33, ALA 46, PHE 103, PHE 105, CYS 106, ASP 109, ALA 153, ASN 154, LEU 156, ALA 166, ASP 167	CYS 106	3.89
4b	-54.67	ILE 25, GLY 28, VAL 33, ALA 46, LYS 48, VAL 79, PHE 103, PHE 105, CYS 106, ASP 109, LEU 156, ASP 167	CYS 106 LYS 48	3.12 3.01
4c	-52.93	ILE 25, GLY 28, VAL 33, ALA 46, LYS 48, VAL 79, PHE 103, PHE 105, CYS 106, ASP 109, LEU 156, ASP 167	CYS 106 LYS 48	3.18 3.09
5a	-49.30	LYS 48 LEU 51 PHE 103 CYS 106 LEU 156 ASP 167	ASP 167	2.58
6a	-41.28	LYS 48 LEU 51 PHE 103 CYS 106 LEU 156 ASP 167		

Journal of Chemical Health Risks
www.jchr.org
JCHR (2024) 14(1), 1111-1120 | ISSN:2251-6727

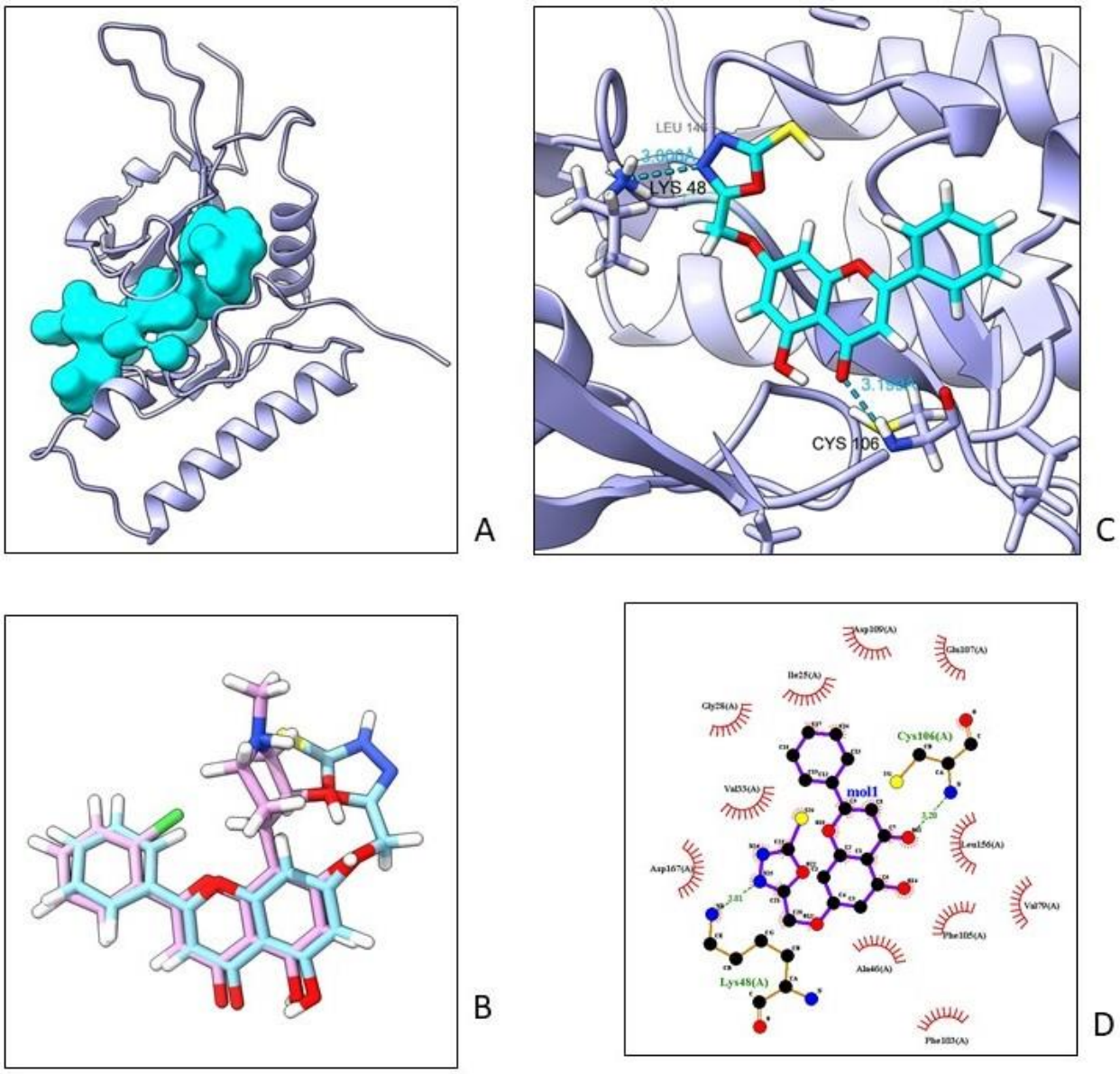

Figure 3. (A.) Receptor's Active Site: Defined as the Region Surrounding the Reference Ligand Flavopiridol (B.) Result of the docking. Crystallographic ligand in Pink and the best docking pose in cyan. (C.) 3D model of the interactions 4b (shown in cyan) and CDK9 at the inhibitor site (D.) 2D model of the interactions 4b (shown in cyan) and CDK9 at the inhibitor site.

5. Conclusion

This study provided comprehensive insights into the synthesis, structural characterization, and biological activity of various derivatives of 7-(2-hydrazineyl-2-oxoethoxy)-5-hydroxyflavone. The IR and NMR spectral data confirmed the successful synthesis of the compounds, with specific markers such as NH and carbonyl stretches, as well as aromatic and methylene protons, indicating the presence of desired functional groups and structural frameworks.

The cytotoxicity assays against breast cancer cell lines MCF-7 and MDA-MB-231 revealed a notable variance in the anticancer activity of the derivatives. Compounds 4a, 4b, and 4c displayed potent activity, particularly against MCF-7 cells, with 4b

Journal of Chemical Health Risks

www.jchr.org

JCHR (2024) 14(1), 1111-1120 | ISSN:2251-6727

and 4c also showing significant effects on MDA-MB-231 cells. This suggests that certain structural features, possibly the pyrazol, oxadiazol, and triazol ring substitution at the C7 position, enhance the compound's ability to interact with the target proteins effectively, leading to increased anticancer activity. In contrast, compounds 5a, and 6a, which lacked cytotoxic effects, underscore the steric hindrance imposed by bulky groups, which can influence the compound's therapeutic potential.

Molecular docking studies provided further understanding of the compounds' interactions with the receptor's active site. The low RMSD values obtained from redocking native ligands and the favorable grid scores of the synthesized Flavone derivatives, particularly compound 4b and 4c highlight their promising binding efficiencies and stable conformations. The significance of hydrogen bond interactions with CYS 106 residues in the receptor's hinge region was also underscored, suggesting a mode of action for the observed anticancer activities.

In conclusion, this study advances the understanding of Flavone derivatives as potential anticancer agents The valuable insights gained from spectral analyses and molecular docking studies contribute to the broader field of medicinal chemistry, guiding future research in the design and development of novel anticancer drugs.

References

1. Ansari A, Agarwal M, Singh VK, Nutan K, Deo S, Deori TJ. 2023 Breast Cancer Literacy: Status of Peripheral Health Workers in Lucknow. Asian Pacific Journal of Cancer Care. 8(2), 287-94.
2. Johnson KS, Conant EF, Soo MS. 2021 Molecular subtypes of breast cancer: a review for breast radiologists. Journal of Breast Imaging. 3(1), 12-24.
3. Thomas NS, Scalzo RL, Wellberg EA. 2024 Diabetes mellitus in breast cancer survivors: metabolic effects of endocrine therapy. Nature Reviews Endocrinology. 20(1), 16-26.
4. Reddy VA, Sarin R, Panda D, Hanitha R, Jain J, Chatterjee S, et al. 2023 A Multi-centric retrospective study into the epidemiological distribution of breast cancer patients in India. Journal of Cancer Research and Therapeutics.
5. Mandal R, Becker S, Strebhardt K. 2021 Targeting CDK9 for anti-cancer therapeutics. Cancers. 13(9), 2181.
6. Fujinaga K, Huang F, Peterlin BM. 2023 P-TEFb: The master regulator of transcription elongation. Molecular cell. 83(3), 393-403.
7. Yamaguchi Y, Inukai N, Narita T, Wada T, Handa H. 2002 Evidence that negative elongation factor represses transcription elongation through binding to a DRB sensitivity-inducing factor/RNA polymerase II complex and RNA. Molecular and cellular biology. 22(9), 2918-27.
8. Lemke J, von Karstedt S, Abd El Hay M, Conti A, Arce F, Montinaro A, et al. 2014 Selective CDK9 inhibition overcomes TRAIL resistance by concomitant suppression of cFlip and Mcl-1. Cell Death & Differentiation. 21(3), 491-502.
9. Mustafa EH, Laven-Law G, Kikhtyak Z, Nguyen V, Ali S, Pace AA, et al. 2023 Selective inhibition of CDK9 in triple negative breast cancer. Oncogene. 1-14.
10. Hu Q, Poulose N, Girmay S, Helevä A, Doultsinos D, Gondane A, et al. 2021 Inhibition of CDK9 activity compromises global splicing in prostate cancer cells. RNA biology. 18(sup2), 722-9.
11. Poon E, Liang T, Jamin Y, Walz S, Kwok C, Hakkert A, et al. 2020 Orally bioavailable CDK9/2 inhibitor shows mechanism-based therapeutic potential in MYCN-driven neuroblastoma. The Journal of clinical investigation. 130(11), 5875-92.
12. Borowczak J, Szczerbowski K, Stec E, Grzanka D, Szylberg Ł. 2020 CDK9: therapeutic perspective in HCC therapy. Current Cancer Drug Targets. 20(5), 318-24.
13. Thieme E, Bruss N, Sun D, Dominguez EC, Coleman D, Liu T, et al. 2023 CDK9 inhibition induces epigenetic reprogramming revealing strategies to circumvent resistance in lymphoma. Molecular Cancer. 22(1), 1-17.
14. Ma H, Dean DC, Wei R, Hornicek FJ, Duan Z. 2021 Cyclin-dependent kinase 7 (CDK7) is an emerging prognostic biomarker and therapeutic target in osteosarcoma. Therapeutic advances in musculoskeletal disease. 13.
15. Santo L, Siu KT, Raje N, editors. Targeting cyclin-dependent kinases and cell cycle

progression in human cancers. Seminars in oncology; 2015: Elsevier.
16. Al-Oudat BA, Alqudah MA, Audat SA, Al-Balas QA, El-Elimat T, Hassan MA, et al. 2019 Design, synthesis, and biologic evaluation of novel chrysin derivatives as cytotoxic agents and caspase-3/7 activators. Drug design, development and therapy. 423-33.
17. Choe H, Kim J, Hong S. 2013 Structure-based design of flavone-based inhibitors of wild-type and T315I mutant of ABL. Bioorganic & medicinal chemistry letters. 23(15), 4324-7.
18. Supino R. 1995 MTT assays. In vitro toxicity testing protocols. 137-49.
19. Prism G. 2020 GraphPad Prism. GraphPad Software Inc.
20. Baumli S, Lolli G, Lowe ED, Troiani S, Rusconi L, Bullock AN, et al. 2008 The structure of P-TEFb (CDK9/cyclin T1), its complex with flavopiridol and regulation by phosphorylation. The EMBO journal. 27(13), 1907-18.
21. Bento AP, Hersey A, Félix E, Landrum G, Gaulton A, Atkinson F, et al. 2020 An open source chemical structure curation pipeline using RDKit. Journal of Cheminformatics. 12, 1-16.
22. Halgren TA. 1996 Merck molecular force field. I. Basis, form, scope, parameterization, and performance of MMFF94. Journal of computational chemistry. 17(5-6), 490-519.
23. Allen WJ, Balius TE, Mukherjee S, Brozell SR, Moustakas DT, Lang PT, et al. 2015 DOCK 6: Impact of new features and current docking performance. Journal of computational chemistry. 36(15), 1132-56.
24. Pettersen EF, Goddard TD, Huang CC, Meng EC, Couch GS, Croll TI, et al. 2021 UCSF ChimeraX: Structure visualization for researchers, educators, and developers. Protein Science. 30(1), 70-82.
25. Wallace AC, Laskowski RA, Thornton JM. 1995 LIGPLOT: a program to generate schematic diagrams of protein-ligand interactions. Protein engineering, design and selection. 8(2), 127-34.